Research Journal of Recent Sciences _____ ISSN 2277-2502
Vol. **4(3),** 68-74, March **(2015)** *Res.J.Recent Sci.*

An anlytical and Numerical solution of Combined Loading in offshore Foundations

Mohammad Sadegh Barkhordari
Bachelor of Civil Engineering, Isfahan University of technology, Isfahan, IRAN

Available online at: www.isca.in, www.isca.me
Received 20th April 2014, revised 30th September 2014, accepted 7th December 2014

Abstract

Todays, Offshore foundations which achieve stability through the putting well in seabed using engineering consideration, are paying considerable attention. By this approuch, in this study combined loading of some kinds of footings studied well to asses the stiffness. Analytical and numerical methods have been applied to have an comparison in this study. Numerical finite element methods have been used and the results showed that numerical solutions have a good agreement with analytical methods and the errors have been reported.

Keywords: Offshore, foundations, combined loading.

Introduction

Curiosity and increasing life needs have always motivvate man to invent and doscover new things , so the results are different broad transformations in modern technologies. exploitnig seas and rivers is one of such human needs to access worthy resources on the planet besides making a commincation with different human habitats. Schorlas of civil engineering thus, have attmepted through larg pool of experiments and experinces and technical knowedge casue fundamental changes in this subject.

To access construction projects as well as providing required mecahical instruments and establishment of prtective equptments to build propoer aqua workshops, civil engeeners have greatly endevoured ended to many significant accomplishmenbts in field of civil engineering. As a matter of fact, activities of underwater workshops operationally relate to sxploration and exploitation of oil and gas besides establishment of under water pipe lines are a matter of high sigciance. The under water foundation system is a method has been utilized in industrial projects espeially in the offshore patforms for establishmen of oil and gas well drilling equipments so far.

Also, for underwater concreting , the direct pomping via termier pipe the concrete maker machinary is utilized. Thris method is used because the goal is to prevent concrete from surounding water.

Foundation in water: The issue of foundation in water (sea and river) from past years till now has always been critical. during the receny years also many considerable achievements have been obtianed in field of foundation in water (under water) and utlizing operational techniques and equipments. For foundation and installing bridge trauss into water, it is required first remove water from the foundation site temporarly. For this operation , it is possible to use from water stream to minor channel and then keep it away from the foundation site temporarily by some walls. The water deviation is usually taken into account only when this operation is geographically possible and also flowing water to other waterway is doable. If for some reason water deviation does not occur, a few other methods will be impmeneted which also need utilizing some equioments withough them in water operation would be impossible. These procedures include as followings:

Sheet pilling: Sheet is made of some steel column or precast concrete plates piled into the ground separately or with integrated parts and are utilized as a barrier against water flow or for turning water and/or protection from the excavation site or the pipe line. These precast steel or cconcerete plates are used in conditions where the excavation site depth does not exceed 15m, otherwise a few other forms of plates will be applicable. These sheets (column plates) are locked by joints on two ends.

Utilizing pick hammer continues untill when the sheets are fixed in a specific depth of the floor level balance and in length of the foundation site which is in a rectangualr or cylinder or charter forms. When the hight of sheets is lower than the specific size, through vulcanize of two or more sheets, the desiredhieght is achived. After this stage, water pomping from inside the site surounded by the sheets will be done. Then, via big rakes the waste materials produced by excavation will be removed. With sp,e machineries on top of the operation room the concerete is injected into the excavation floor in order to prevent from pentration of water beaneath the machinary is casued by.

Injection of concerete is done via a long pipe with a wide open mouth and a funnel on top of it . it shold be mentioned here that

injonection of concrete must be permanent and in all areas of the concrete injection , the pipe shold be continously circulates in lonigitudinal and transverse directions so that prohibits from concrete to get dry. When conrete injection finished , the penetration water should be pomping the sourinding water may break steel plates because of external water pressure and consequently pressure difference among two areas. In this condition, long and thick bars are controled by vertical tapes outside the operation room by the resistant bars are utilized.

It should be mentioned that deeper water in the operation site will increase usage of the timbers. after water pumping which , istallation of the pre-designed foundation or waterfront will initiates. Then the process of rebar investment, formating, and concreting begine. After concerete injection was finished leave it to dry and gets ready. Finally, the wooden molds and material sheets are previously installed will be dismantled. Attnetion that if you want to directly move them or evict, all operation will be ruined because of water pressure.

So, to prevent this, one or more holes water must be inserted into the site in order to re-fill it and backs it to pre-pumping stage. When this stage finished completely the steel plates could be drawn out underwater and ends the process.

Methodology

Wave Characteristics: The wave characteristics; wave height, wave period were deduced from relevant meteorological and oceanographic studies[1,2] while wave celerity, c, and wave length, L, were evaluated for conditions of shallow water waves[3].

Hydrodynamic Coefficients: Inertia coefficients, Cm, and drag coefficient, Cd, are reported to generally lie in the range of 0.8 to 2.0[4] and there values are usually obtained from standard charts. However, Akpila and Ejezie have reported that these coefficients have Cm of 1.5 and Cd of 0.7 in the offshore Niger Delta. The dimensionless parameters for maximum drag force, KDm, inertia force, Kim, maximum drag moment, SDm, and maximum inertia moment, Sim, were evaluated from standard charts[5].

Hydrodynamic Forces: The total instantaneous hydrodynamic force, F, on a submerged structure per elemental length, ds of the cylinder can be is obtained from the expression;

$$F_d = \frac{C_d}{2}\rho_w D^2 + C_m\rho_w\left(\pi\frac{D^2}{4}\right)\frac{2\pi^2 H}{T^2}\left[\frac{\cosh\, k(d+z)}{\sinh kd}\right]\sin(kx-\omega t) \quad (1)$$

While the maximum horizontal force is obtained by summing both the drag force and inertia force as follows:

$$F_d = \frac{C_d}{2}\gamma_w D H^2 K_{Dm} + C_m\gamma_w\left(\pi\frac{D^2}{4}\right)HK_{im} \quad (2)$$

where F is horizontal force, γ_w is unit weight of water, D is pile diameter, ρ_w is density of water and H is wave height.

Concentric vertical loads: The renowned methods of Brinch Hanson and Vesic were adopted for cases with the ratio of foundation depth to breadth, Df/B≤1.0 and Df/B≥1.0[6-7]

Vertical and Horizontal Load (M = 0): The expression for a rectangular foundation subjected to combined vertical-horizontal load (4) is given as;

$$\frac{V_u}{A} = (2+\pi)S_u\left(1+\frac{B'/L'}{2+\pi}\right)\left(1-\frac{\frac{2+B'/L'}{1+B'/L'}H}{(2+\pi)S_u B'L'}\right) \quad (3)$$

Where: $B'$and $L'$are the dimensions of the fictitious effective area $A'$of the foundation, S_u is undrained shear strength of soil, Vu is maximum vertical load and H is wave height. For the case of $B' = L'$Equation (3) becomes;

$$\frac{V_u}{As_u} = 1.2\left[(2+\pi) - \frac{3H}{2As_u}\right] \quad (4)$$

and the maximum horizontal load (Ho) is given by;

$$H_0 = As_u = \left(\frac{1}{2+\pi}\right)V_0 \quad (5)$$

Where: sliding failure is incipient at V/Vo < 0.5. A recent study on the performance of foundations under vertical load induced displacement in the off shore has been reported.

A maximum directional wave height, H max of approximately 7.0 m, mean wave period of 17 sec and average wind speed of 14.1m/s were obtained.

Analytical Surface Footing Solutions: Most of the available elastic solutions refer to footings placed at the ground surface. The main reference for elastic solutions in soil mechanics is Poulos and Davis[8]. Four closed-form solutions are given on pages 166 and 167 of this book for a rigid circular flat footing at the surface of an elastic half-space subjected to vertical, horizontal, moment and torsional loads.

Examination of the derivation and boundary conditions of these solutions has shown that two refer to a smooth footing, one refers to a rough footing and the other is not exact. This section separates these and other solutions into smooth and rough footing categories for which six cases in total exist.

For the combined loading problem under consideration, the stiffness of loading can be written in the following matrix from in terms of four non-dimensional coefficients, K1-K4:

$$\begin{bmatrix} V/GR^2 \\ H/GR^2 \\ M/GR^3 \end{bmatrix} = \begin{bmatrix} K_1 & 0 & 0 \\ 0 & K_2K_4 & \\ 0 & K_4K_3 & \end{bmatrix}\begin{bmatrix} u_V/R \\ u_H/R \\ \theta_M \end{bmatrix} \quad (6)$$

For a rough surface footing, K1 can be obtained from the equation but there is no exact solution for K2, K3 and K4 except for incompressible soil condition.

It is important that for incompressible undrained soil, the K4 is zero. So, K2 and K3 can be obtained from above matrix.

Mesh Dimensions and Topology: Application of the finite element method to footing analysis has largely concentrated on the plastic response and prediction of vertical collapse loads. In these analyses the mesh dimensions were generally of the order five times the width of the footing, or in the case of a circular footing, ten times the radius (10R). These exact mesh dimensions were adopted by sloan in his analysis of smooth rigid strip circular footings. Using the appropriate finite element formulations, exact collapse loads were predicted to within 1% accuracy. However, the initial tangent of the load-displacement curves showed a repeatable 10% over prediction of the initial elastic stiffness.

Table-1 demonstrates this over prediction to be a consequence of the closeness of mesh boundaries to the footing.

The effect of mesh dimensions on the accuracy of elastic footing analysis, presented in table-1., was analyses using a mesh of 6-node triangular elements and program OXFEM (oxford soil mechanics two-dimensional finite element model). The problem of a vertically loaded smooth rigid circular footing placed at the surface of an elastic compressible half-space (v=0.25) was considered for which an exact solution. For a footing of radius R, two-dimensional meshes of dimensions 10R×10R, 50R×50R and 200R×200R were refined until no further significant improvement in numerical accuracy was achieved. For each mesh, the error in vertical stiffness, presented in table 1, is calculated using equations below.

$$\text{Error}(\%) = \frac{K_p - K_e}{K_e} \times 100 \qquad (7)$$

Table-1
The effect of mesh dimensions on the accuracy of elastic footing analysis

Mesh dimensions(D*D)	R/D (%)	Number of nodes	Number of elements	Error in stiffness
10*10	10.5	400	230	9.8
50*50	1.8	550	290	2.5
200*200	0.3	700	340	0.9

Table-1 demonstrates that the error in numerical prediction decreases significantly with an increased mesh dimension (D). It can be shown for a point load that the error due to a finite boundary, in this case a mesh boundary, is inversely proportional to the distance to the fixed boundary. For a circular footing, this can be approximated by the non-dimensional parameter R/D, and is thought to become more applicable the greater the distance from the footing to the boundary. The parameter R/D , expressed as a percentage, is included in table 1 and compares well with the observed errors, the latter being on average 0.3% greater. This difference may be due to discretization errors in the finite element mesh close to the footing, which are not affected by the mesh dimension.

All three-dimensional surface footing elastic analyses presented in this section use the 20-node quadratic strain tetrahedron mesh, which has mesh dimension of 200R. Taking into account the results of table 1, the error in stiffness due to the proximity of the mesh boundaries is estimated to be of the order +0.3% , adopting a larger mesh dimension, and therefore a larger number of nodes and elements, is considered inefficient as the small improvement in accuracy does not compensate for the increased computational effort. Notes that in mesh ESS20, special care was taken to pack a high density of elements under edge of the rigid footing where high stress and strain gradients occur. Also note the extreme gradation of very small elements close to the footing to large elements near the boundary of the mesh.

Numerical Integration for the 20-node Tetrahedron: The commonly used finite element texts by Zienkiewicz and Kardestuncer and Norrie advocate the use of a 5-point Gaussian integration scheme for the numerical integration of the stiffness matrix for the 20-node quadratic strain tetrahedron adopted in this study. This scheme involves a negative weighting of -0.8 at the centroid of the tetrahedron. While this scheme is exact when integrating functions up to order 3, it produces spurious solutions when terms of a higher order exist, as is the case in the finite element methods[9-10]. Zienkiewicz and kardenstuncer and Norrie make no mention of this limitation of the 5-point scheme, however, Gens et al do note the detrimental effect of a negative gauss point weighting[11].

An alternative 8-point scheme for tetrahedral, exact to order 3 (quadratic strain), has been developed by Abramowitz and Stegun and is used in this research. It has positive weightings and integration points located at the corners and centroid of each triangular face. The location of the gauss points at the surface of the element proves most advantageous when processing the stress data[12].

Results and Discussion

The analytical solutions for vertically loaded smooth and rough footing are plotted in the non-dimensional form $V/(G\ R\ u_v)$ against poisson's ratio (v) in figure-1 and are compared with numerical results at discrete values of v. For both rough and smooth conditions, the numerical results compare well, with the error being in the range +2.5% to +3.9% for v = 0.0 to 0.49. the smooth and rough analytical solutions show the stiffness of rough footing to be about 10% greater than the smooth footing at v = 0.0. For undrained soil conditions, v = 0.5, the analytical solutions are the same, and are well reproduced bye the

numerical solutions when v = 0.49 is used in the numerical analysis.

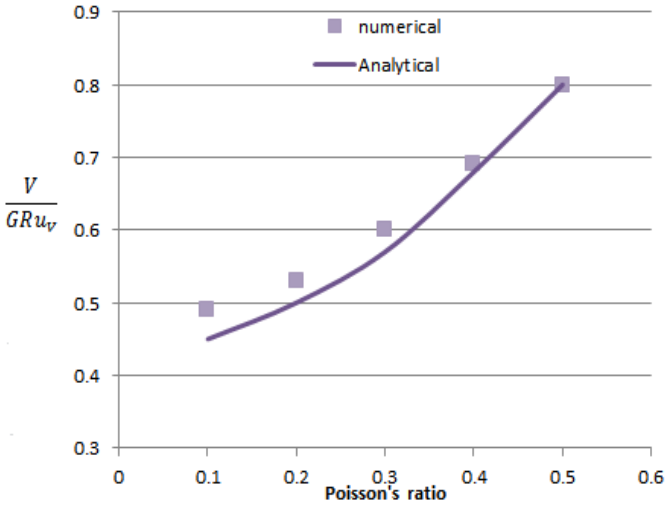

Figure-1
Results of elastic vertical loading analysis of a surface footing

For moment loading of a footing, the exact analytical solution is compared with the numerical results in figure-2. The results are expressed in terms of the non-dimensional stiffness parameter $M/(G\ R^3\theta_M)$. The errors in the numerical solutions are in the range +2.5% to +3.4%, this being very similar to those observed in the vertical loading case.

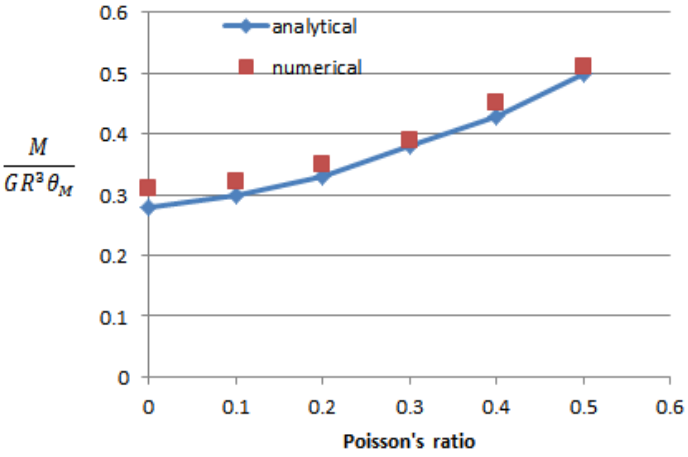

Figure-2
Result of elastic moment loading analysis of surface footing

As discussed in section before, the horizontal and moment loading cases are cross coupled for a rough footing. This cross relationship can be expressed either as the loads in terms of the deformations (stiffness), or the deformations in terms of the loads (flexibility). It is far easier in finite element analysis to prescribe the footing node displacements for a rigid body displacement than to use load control. Therefore, the numerical analysis of this section adopted the procedure suggested in last section for evaluating the stiffness coefficiens K_2 , K_3 , K_4. That is, the problems of rigid horizontal displacement and rigid footing rotation were examined, for which the results are presented in table-2. It is pleasing to see that cross coefficient k_4 is the same to 4 significant figure for the displacement and rotation analyses.

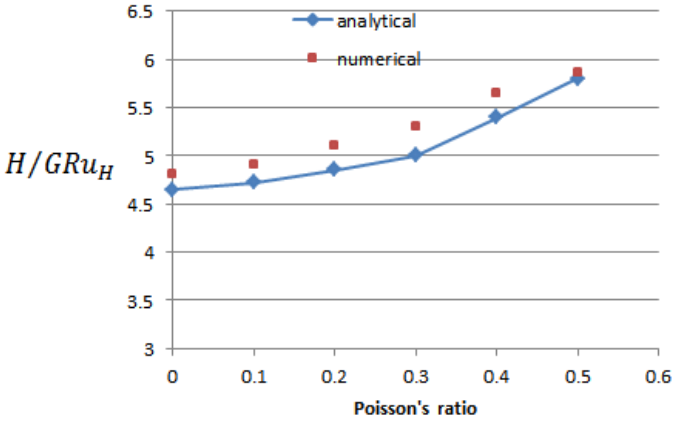

Figure-3
Result of elastic horizontal loading analysis of surface footing

These inferred results for horizontal and moment loading are also included in table-2. One of the main features of these results is the cross coupling between the horizontal displacement (u_H) and body rotation (θ_M) for horizontal and moment loading.

Table-2
Numerical results of horizontal and moment loading of surface footing

v	$\frac{H}{GR^2u_H}$ (=K2)	$\frac{M}{GR^3\theta_M}$= K3
0	4.1	3.1
0.1	4.3	3.5
0.2	4.62	3.71
0.3	4.81	4.2
0.4	5.2	4.65
0.5	5.41	5.4

Where $u_{v_{edge}}$ is the maximum vertical edge displacement corresponding to the rotation θ_M. Similarly for pure moment loading (H=0), the following relationships result.

The ratios $u_{v_{edge}}/u_H$(horizontal loading) and $u_H/u_{v_{edge}}$ are included in table-2. These results show a significant coupling between $u_{v_{edge}}$ (θ_M) and u_H for low values of poisson's ratio and no coupling as v=0.5, applicable to undrained clay, is approached. For values of poisson's ratio representative of a drained sand, v≈0.2, the ratios $u_{v_{edge}}/u_H$ and $u_H/u_{v_{edge}}$ are in the range 11.5-15%.

These results can be interpreted as follows. A horizontally loaded footing on drained sand will elastically rotate about a horizontal axis perpendicular to the direction of the applied load, and the corresponding maximum vertical edge displacement in this plane will typically be about 15% of the total horizontal displacement. As demonstrated before, current elastic solution do not take into account this cross coupling, which is additive for the case when the moment arises from a horizontal load applied at some distance above the footing, as is applicable to offshore foundations. However, by comparison with the errors involved in determining representative elastic soil parameters, this cross coupling effect is thought not be significant in most cases for a surface footing. Therefore the following comparisons of numerical and analytical elastic solutions for moment and horizontal loading of a surface footing do not take the cross coupling into account.

The numerical results for a rough footing subjected to moment loading are also presented in figure 2. These results are expressed as $M/(G R^3\theta_M)=1/F1$, where F can be expressed as follows:

$$F_1 = \frac{K_2}{K_2K_3 - K_4^2} \quad (8)$$

Since the derivation of the analytical solutions is intended in a flexibility. The difference in response between the smooth and rough footings varies from 13% for v=0.0 to zero for undrained conditions, v=0.5. This difference represents the error associated with modeling the response of a rough footing, subjected to moment loading.

For a rough footing loaded horizontally, the numerical solution relating the horizontal load (H) to the horizontal displacement (u_H) is given in figure 3 and compared with two approximate analytical solutions. The results are expressed in terms of the non-dimersional parameter $H/(G Ru_H)=1/F_2$, where F2 can be expressed as below:

$$F_2 = \frac{K_3}{K_2K_3 - K_4^2} \quad (9)$$

Any comparison should take into account the observed errors between the finite element and exact solutions for the vertical and moment loading cases considered previously. It is therefore concluded that the Gerrard and Harrison solution, although approximate, provides a very good estimate of the true response for the full range of poisson's ratio considered[13]. The Bycroft solution is seen to provide a poorer estimate for values of poisson's ratio considerably less than 0.5[14].

Comparison with available solutions for vertical loading: We assume three models of rigid rough circular footing. It showed in below figure the putting surfaces in water.

For a footing located at the bottom of a trench (Model 1), the ratio of the vertical stiffness of the footing (K_{1emb}) to the vertical stiffness of an equivalent surface footing (K_{1swf}) is plotted against the depth of embedment in figure 5. Presenting the results as the ratio K_{1emb}/K_{1swf} represents the reduction in footing settlement due to embedment and has the advantage that the ratio removes many of the discretization errors inherent in the finite element method. It also allows easy comparison of the numerical results with the empirical solution of Gazetas et al (1985).[15] This equation is rewritten below in terms of the vertical stiffness ratio

K_{1emb}/K_{1swf} .

$$\mu_{trench} = 1 - 0.08\frac{h}{R} \quad (10)$$

$$\mu_{wall} = 1 - 0.23(\frac{h}{R})^{0.54} \quad (11)$$

Where h is the depth of the footing surface in the water and is included in figure-5 for Model 1 ($\mu_{wall} = 1.0$). Figure-5 shows the Gazetas et al (1985) solution, which is assumed to be independent of poisson's ratio (v), compares poorly with the numerical solutions, which demonstrate the increase in vertical embedment stiffness to be significantly dependent on v. The finite element results also demonstrate that the incremental increase in vertical stiffness becomes smaller with embedment depth, as would be expected.

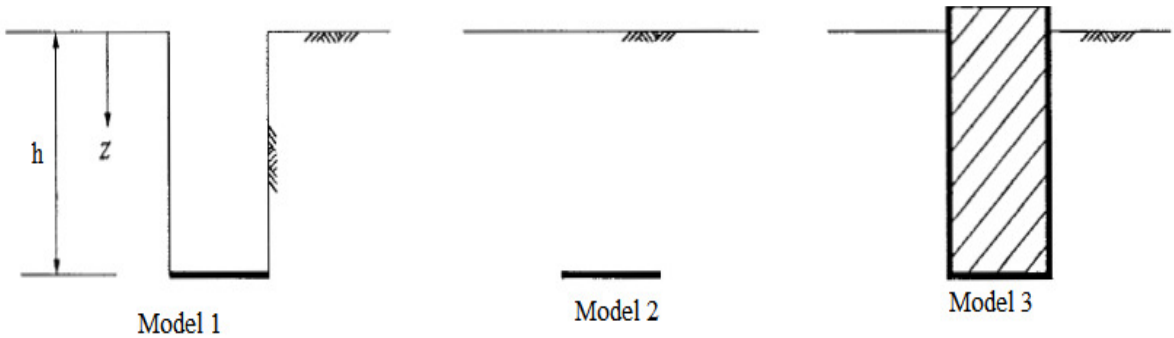

Figure-4
Model1 is the bottom of a trench, Model 2 is a covered footing and the Model 3 is full sidewall contact

Butterfield and Banerjee, present boundary element solutions for a vertically loaded rigid circular footing embedded below the surface of an isotropic homogeneous half-space for values of v=0.0, and 0.5. The boundary conditions are equivalent to Model 2, a covered footing, except that footing surface is assumed to be smooth, while in this study it is taken to be rough. The Butterfield and Banerjee solution demonstrate that with deep embedment the ratio K_{1emb}/K_{1swf} approaches constant values of about 2.5 and 2 for v=0 and 0.5 respectively, and that a large proportion of the embedment effect is generated by a depth of 8R. For the embedment depth range examined in this study, these solutions are compared in figure 6 with the finite element solutions for a covered footing. In general, the two sets of solutions compare well. For v=0.0, the 10% difference in the curves is attributed to the differing smooth and rough boundary conditions. The solutions are much closer under incompressible soil conditions (v=0.5). This is as anticipated since the vertical stiffness of rough and smooth surface footings are the same when v=0.5[16].

The Gazetas et al solution is also applicable to the problem of an embedded footing with full sidewall contact (Model 3). As for figure 6, this solution, expressed as the stiffness ratio K_{1emb}/K_{1swf}, is compared with the numerical results in figure-7. The finite element solution shows the increase in embedment stiffness to be dependent on v and that the gazetas et al solution agrees closely with this for $z_D/R = 0.0 - 2.5$ and v=0.4. This is a promising result as the Gazetas et al solution is intended for poisson's ratio values in the range 0.25 to 0.5.

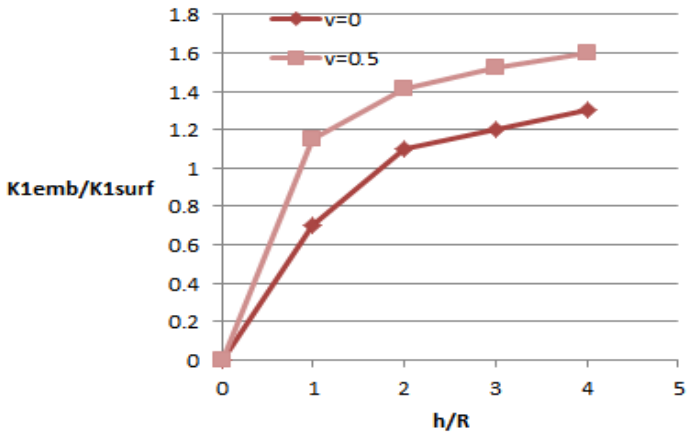

Figure-5
The increase in vertical stiffness due to embedment for a footing at the bottom of the trench

Conclusion

The elastic behavior of offshore foundations has important applications to many aspects of offshore design. For a rigid circular footing, most of the available elastic solutions refer to footings placed at the surface level. Exact solutions exist for the two possible loading cases of a smooth surface footing, that is, vertical and moment loading. For a rough footing, the vertical loading case has an exact solution, while the only other available solutions approximate horizontal loading. These approximate solutions fail to recogise the cross coupling between the horizontal load moment responses for a rough surface footing.

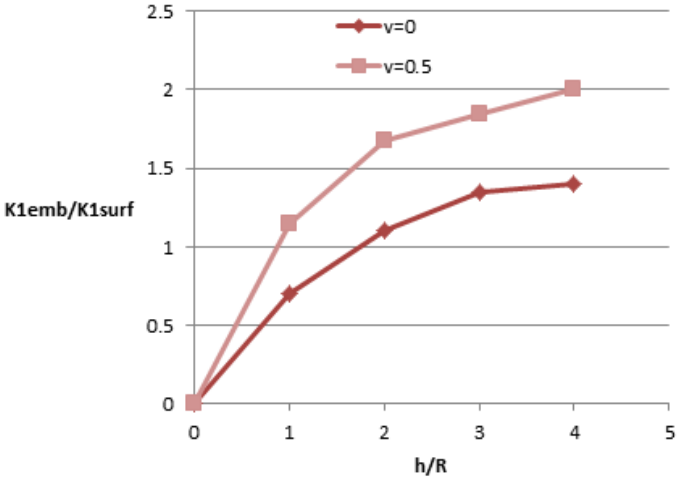

Figure-6
The increase in vertical stiffness due to embedment for a covered footing

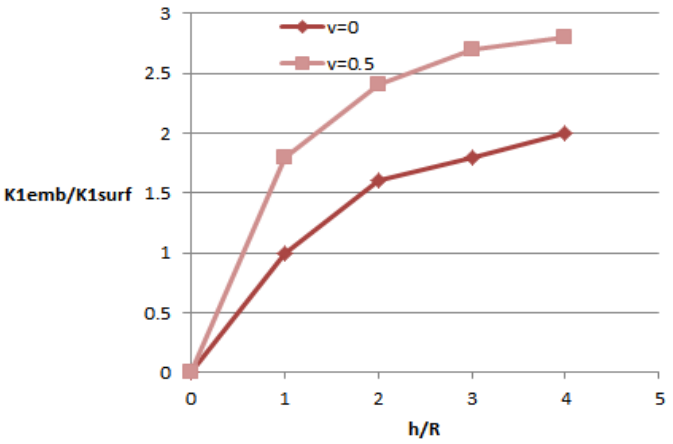

Figure-7
The increase in vertical stiffness due to embedment for a footing with fuul sidewall contact

Finite element analyses of a rigid circular footing placed on an elastic continuum demonstrated that the proximity of the mesh boundaries can affect the accuracy of the elastic stiffness prediction. A mesh dimension of 200 footing radii (R) was therefore adopted for all elastic analyses reported, and is thought to limit the error to about +0.5%. For a surface footing, the exact analytical solutions are well reproduced by the numerical solutions. The numerical solutions also show that the cross coupling between the horizontal load and moment components is in most cases not very significant for a rough surface footing, and is non-existent for an incompressible soil. Numerical

comparisons with two approximate horizontal loading analytical solutions demonstrated that one solution provides a good estimate of the true response, while the other gives a poorer estimate for compressible soils.

The effect of footing embedment on the elastic response was investigated to embedment depths of 4R, for combined loading conditions, and the full range of poisson's ratio. Three cases of (rough) footing embedment were numerically examined: i. footing at the bottom of a trench, ii. covered footing, and iii. embedded footing with full side wall contact, for which the vertical, horizontal, moment and cross coupling stiffness coefficients were computed. Comparison with readily available and usable analytical and numerical solutions was limited to the vertical loading case. This is some cases verified the finite element solutions, and in other cases highlighted possible limitations in the empirical equations of Gazetas et al.

Closer examination of the embedment results was performed in terms of the ratio of the embedded footing stiffness to an equivalent surface footing stiffness. This ratio effectively represents the reduction in footing displacement (or rotation) due to embedment. The results clearly show that a footing with full sidewall contact has a greater increase in stiffness with embement than a covered footing, and that a covered footing has a greater increase than a footing at the bottom of a trench. The latter two cases of footing embedment approach a constant value of stiffness with embedment depth, while a footing with full side wall contact approaches a constant gradient of increasing stiffness. For the horizontal and moment loading cases, the influence of embedment on footing stiffness is developed at shallower depths than vertical loading, with an appreciable reduction in horizontal displacement and rotation being observed by an embedment depth of one footing radius.

References

1. Santala M.J.., Eastern Nigerian Shallow Water Metocean Criteria, 1.2, **(2002)**

2. Cooper, Met Ocean and Hydrodynamic Criteria for Shallow fixed Structures and Pipelines off W. Africa, Revision 11 **(2004)**

3. Sorenson R.M., Basic Coastal Engineering, 3th edition, Spring Science and Business media, New York, **(2006)**

4. Haritos N., Introduction to the analysis and design of offshore structures : An overview, EJSE, Special Issue : Loading in Structures, 55-65 **(2007)**

5. Akpila S.B. and Ejezie S.U., *International Journal of Current Research*, **3(10),** 087-091 **(2011)**

6. Brinch Hanson J., A revised and extended formula for bearing capacity, Bull. No.28, the Danish Geotechnical Institute, Copenhagen, 5-11 **(1970)**

7. Vesic S., Bearing Capacity of Shallow foundation, Engineering Handbook, Ed. by H.F. Winterkornand H.Y. Fang, Van Nostrand Reinhold, New York, USA, 121-147 **(1975)**

8. Davis E. H. and Booker J.R., The effect of increasing strength with depth on the bearing capacity of clays, *Geotechnique* **23(4),** 551-563 **(1973)**

9. Zienkiewicz O.C., The finite element method, 3rd edn., McGraw: Hill, Maidenhead, **(1977)**

10. Kardenstuncer H. and Norrie D.H., Finite element Hanadbook, McGraw-Hill, **(1987)**

11. Gens A., Carol I. and Alonso E.E., An interface element formulation for the analysis of soil-reinforcment interaction, *Computers and Geotechnics*, **7,** 133-151 **(1989)**

12. Abramowitz M. and Stegun I.A., Handbook of mathematical functions, National Bureau of Standards, **(1964)**

13. Gerrard C.M. and Harrison W.J., Circular loads applied to a cross-anisotropic half space, C.S.I.R.O. Aust. Div. App. Geomech., *Tech. Paper*, **8, (1970)**

14. Bycroft R.N., Forced vibrations of a rigid circular plate on a semi- infinite elastic space and on an elastic stratum, *Phil. Trans. Roy. Soc.* A., **248,** 327-368 **(1956)**

15. Gazets G., Tassoulas J. L., Dobry R. and O'Rouke M.J., Elastic settlement of arbitrary shaped foundations embedded in half-space, *Geothenique,* **35(3),** 339-416 **(1985)**

16. Butterfield R. and Banerjee P.K., A rigid disk embedded in an elastic half space, *Geot. Engng.,* **2,** 35-52 **(1971)**